HHS Public Access

Author manuscript

Neuroscience. Author manuscript; available in PMC 2015 November 11.

Published in final edited form as:

Neuroscience. 2009 January 23; 158(2): 798–810. doi:10.1016/j.neuroscience.2008.10.017.

Estrogen receptor-α immunoreactive neurons in the brainstem and spinal cord of the female rhesus monkey: species-specific characteristics

Veronique G.J.M. VanderHorst[1,2], **Ei Terasawa**[3], and **Henry J. Ralston III**[4]

[1] Dept. of Neurology, Beth Israel Deaconess Medical Center, Harvard Medical School, Boston, MA 02215, USA [2] Dept. of Pathology and Laboratory Medicine, University of Groningen Medical Center, Groningen, 9700 RB, Netherlands [3] Wisconsin National Primate Research Center, University of Wisconsin, Madison, WI 53715, USA [4] Dept. of Anatomy, University California San Francisco, San Francisco, CA 94143, USA

Abstract

The distribution pattern of estrogen receptors in the rodent CNS has been reported extensively, but mapping of estrogen receptors in primates is incomplete. In this study we describe the distribution of estrogen receptor alpha immunoreactive (ER-α IR) neurons in the brainstem and spinal cord of the rhesus monkey.

In the midbrain, ER-α IR neurons were located in the periaqueductal gray, especially the caudal ventrolateral part, the adjacent tegmentum, peripeduncular nucleus, and pretectal nucleus. A few ER-α IR neurons were found in the lateral parabrachial nucleus, lateral pontine tegmentum, and pontine gray medial to the locus coeruleus. At caudal medullary levels, ER-α IR neurons were present in the commissural nucleus of the solitary complex and the caudal spinal trigeminal nucleus. The remaining regions of the brainstem were devoid of ER-α IR neurons. Spinal ER-α IR neurons were found in laminae I-V, and area X, and were most numerous in lower lumbar and sacral segments. The lateral collateral pathway and dorsal commissural nuclei of the sacral cord and the thoracic intermediolateral cell column also contained ER-α IR neurons. Estrogen treatment did not result in any differences in the distribution pattern of ER-α IR neurons.

The results indicate that ER-α IR neurons in the primate brainstem and spinal cord are concentrated mainly in regions involved in sensory and autonomic processing. Compared to rodent species, the regional distribution of ER-α IR neurons is less widespread, and ER-α IR neurons in regions such as the spinal dorsal horn and caudal spinal trigeminal nucleus appear to be less abundant. These distinctions suggest a modest role of ER-α in estrogen-mediated actions on

Correspondence to: Veronique VanderHorst, Dept. of Neurology, Beth Israel Deaconess Medical Center, Kirstein 406, 330 Brookline Ave, Boston, MA 02215 Phone: 617 677 7000; E-mail: vvanderh@bidmc.harvard.edu.

Section Editor: Dr Charles R Gerfen

primate brainstem and spinal systems. These differences may contribute to variations in behavioral effects of estrogen between primate and rodent species.

Keywords

primate; sensory; autonomic; pain; reproduction; sex steroid

Estrogen modulates neural activity related to a wide variety of physiological events, such as reproductive behaviors (Ogawa et al., 1998), lactation, maternal behaviors, vocalization (Geyer and Barfield, 1978), aggressive behavior (Ogawa et al., 1996), autonomic functions (Saleh et al., 2000), analgesia (Bodnar, 2002), levels of motor activity (Ogawa et al., 2003), food intake (Geary et al., 2001), memory and cognitive functions (Fink and Sumner, 1996, Sherwin, 2000). The above functions are under control of estrogen sensitive hypothalamic and forebrain regions, though modulation takes place via brainstem and/or spinal cell groups. Examples are food intake being modulated by the nucleus of the solitary tract (NTS), cognitive functions by the dorsal raphe nucleus (DRN), vocalization and reproductive behavior by the periaqueductal gray (PAG), and nociception by the spinal dorsal horn and the ventromedial medulla (see VanderHorst et al., 2005).

Most of the data on the effects of estrogen on physiological functions has been obtained in rodents. The few reports involving primates have shown that reproductive behavior and nociception are not modulated by estrogen as much as seen in rodents (Chambers and Phoenix, 1987; Negus et al., 2004), and the same may be true for other actions that are modulated by estrogen. The neuronal basis underlying this differential effect of estrogen on physiological functions is not well understood, but may include differences in the ability of brainstem and spinal neurons to respond to estrogen.

Estrogen-induced behavioral effects might be mediated by populations of neurons that express estrogen receptors. A number of estrogen receptors have been identified, which may mediate their action via genomic and/or non-genomic mechanisms (for review see Vasudevan and Pfaff, 2008). Estrogen receptors-alpha and –beta (ER-α and ER-β) are most abundant in the nucleus though they can also be found at extra-nuclear sites. In addition, recently a possible role in estrogen-mediated actions has been described for the G protein-coupled receptor 30 (GPR30), which is located in plasma membrane, Golgi apparatus and endoplasmic reticulum (Revankar et al., 2005; Thomas et al., 2005; Noel et al., 2008; for review see Vasudevan and Pfaff, 2008).

The distribution of neurons expressing the nuclear estrogen receptors (ER-α and ER-β) in the rodent CNS has been mapped extensively by immunohistochemical or *in situ* hybridization methods (Simerly et al., 1990, Turcotte and Blaustein, 1993, Shughrue et al., 1997, Boers et al., 1999, Merchenthaler et al., 2004, VanderHorst et al., 2005). In the rodent brainstem and spinal cord, large numbers of neurons express ER-α, whereas few neurons express the high affinity isoform of ER-β (Merchenthaler et al., 2004, VanderHorst et al., 2005). The distribution of GPR30 immunoreactive neurons has been recently described in the rat CNS, including midbrain and medulla oblongata (Brailoiu et al., 2007).

The above rodent studies showed some species differences in the distribution patterns of ER-α IR neurons, especially at the level of the brainstem. It is likely that there are substantial species differences between the primate and rodent brainstem. Only a few reports deal with the distribution of estrogen concentrating neurons throughout the CNS in primates (using autoradiographic techniques: Keefer and Stumpf, 1975, Pfaff et al., 1976). More recent studies in the primate, using *in-situ* hybridization or immunohistochemical techniques, focus on hypothalamic and forebrain areas (Herbison et al., 1995, Register et al., 1998, Blurton-Jones at al., 1999), the periaqueductal gray (PAG, ER-α; VanderHorst et al., 2002b), dorsal raphe nucleus (DRN; ER-β: Gundlah et al., 2000, Gundlah et al., 2001) and locus coeruleus (Pau et al., 2000). The distribution pattern of ER-IR neurons in the rest of the primate brainstem and the spinal cord has not been reported in detail. Such information is essential if we are to understand how and to what extent estrogen, acting via estrogen receptors, is involved in the modulation of brainstem and spinal circuitries in primates.

Here we report the distribution of ER-α IR neurons in the midbrain, brainstem and spinal cord of the adult female rhesus monkey. For inter-species comparison, methodology and tissue analysis was similar to a recent study on the distribution of ER-α IR neurons in the mouse (VanderHorst et al., 2005).

Experimental procedures

Animals and surgical procedures

Seven adult female rhesus monkeys (*M. mulatta*; weight: 4.7-7.5 kg; age 8 to 26 years, average age 15 years; cases M11, M12, and M14 to M18) were used (see Table 1 for details). The protocol for this study was reviewed and approved by the Animal Care and Use Committee, University of Wisconsin, Madison, and all experiments were performed under the guidelines established by the NIH and USDA (NIH Guide for the Care and Use of Laboratory Animals; NIH Publications No.80-23). All animals have been included in other studies (VanderHorst et al., 2000a, VanderHorst et al., 2000b, VanderHorst et al., 2001b, VanderHorst et al., 2002a, VanderHorst et al., 2002b, VanderHorst et al., 2004).

To eliminate variations in immunostaining related to variations in menstrual cycle, ovariectomies had been performed in all cases, except for one monkey (M18). Given her age of 26 years as well as based on a menstrual record, the endocrine status of this monkey was postmenopausal. Ovariectomies were performed well in advance of the euthanization of the animals (6 weeks: M11 and M12; 3 months: M16 and M17; more than a year: M14 and M15). Three animals received daily subcutaneous injections of estradiol benzoate (M14, M16, M17; 40μg; Sigma, St. Louis, Mo) for 14 days prior to sacrifice. This dose is sufficient to facilitate mating behavior in female rhesus monkeys (Chambers and Phoenix, 1987). The 3 estrogen treated cases were included to examine whether 14 days of estradiol benzoate treatment would affect the distribution of ERα-IR staining.

At the time of euthanasia the animals were anesthetized with ketamine (10-15 mg/kg; i.m.) and pentobarbital (25-30 mg/kg; i.v.), and transcardially perfused with 2 liters of phosphate buffered saline (PBS; pH 7.4; 0.1M; room temperature) followed by 2 to 3 liters of fixative. The fixative contained 0.5% glutaraldehyde (EMS, Fort Washington, PA) and 4%

paraformaldehyde (EMS, Fort Washington, PA) in 0.1M phosphate buffer (pH 7.4; cases M11 and M12), 1.5% glutaraldehyde and 1.5% paraformaldehyde (cases M14 to M17), or 4% paraformaldehyde (M18). The high glutaraldehyde fixation in M14 to M17 was necessary for tracing experiments that were conducted in these animals as part of other studies (VanderHorst et al., 2000a, VanderHorst et al., 2002b).

The CNS was removed, post-fixed for 2-4 hours, and stored in PBS (M11 to M17) or 25% sucrose in PBS (M18; both at 4° C). The midbrain, brainstem and spinal segments C1, C3, C7, T2, T12, L2, L4, L5, L6, L7, S1, S2, and S3 were blocked and each block was cut into 10 series of 50μm sections on a vibratome (M11 to M17) or a freezing microtome (M18).

ER-α immunohistochemistry

For visualization of ER-α IR neurons, 2 primary antibodies were used. The H222 antibody (gift by Abbott Laboratories, Chicago, Ill.; 1.0 μg/ml, 1:1000) is directed against the ligand-binding domain of ER-α. The specificity of the H222 antibody has been documented previously (see King and Greene, 1984). Using the H222 antibody, the distribution of ER-mRNA and ER-IR was similar in the rhesus monkey hypothalamus (Bethea et al., 1996). Theoretically, the H222 antibody might also detect ER-β. Therefore, an additional experiment was performed using the 1D5 antibody (monoclonal mouse anti-human estrogen receptor; DAKO, Denmark; 230μg/ml at a dilution of 1:400), which is directed against the N-terminus of ER-α, a region that does not overlap with ER-β. In rat (Greco et al., 1998) and monkey (VanderHorst et al., 2002b) the distribution of ER-IR neurons in the CNS is similar with these 2 antibodies. Moreover, ER-beta mRNA is presents in the substantia nigra, caudal linear nucleus, dorsal raphe nucleus and pontine nuclei (Gundlah et al., 2000). Our material includes these regions, but no immunoreactivity was found in these regions using the H222 antibody.

The procedure that was used to visualize ER-IR neurons has been extensively described previously (VanderHorst et al., 2002b). Briefly, for visualization of ER-α with H222, the tissue was cut into 10 series of transverse sections at 50μm thickness on a vibratome, one series of which was used for the present study. After pretreatment with 1% sodium borohydrate to remove excess aldehydes, free-floating sections were incubated with H222, followed by biotinylated sheep anti-rat immunoglobulin (Amersham Pharmacia Biotech Inc., Piscataway, NJ), and avidin-biotin-complex-peroxidase (ABC, Vectastain, Vector Laboratories, Burlingame, CA; diluted 1:100). For visualization of ER-α with 1D5, the tissue was cut into 10 series of 50μm sections on a freezing microtome. Free-floating sections were incubated in 1D5, followed by biotinylated horse anti-mouse immunoglobulin (1:200; Vector, Vector Laboratories, Burlingame, CA), and avidin-biotin-complex-peroxidase (ABC, Vectastain, Vector Laboratories, Burlingame, CA; diluted 1:400). A blue-black reaction product was obtained enzymatically with diaminobenzoate and nickel ammonium sulfate. The sections were mounted on slides, dehydrated in a graded series of alcohol, and coverslipped with DePeX mounting medium (EMS, Fort Washington, PA). Selected series were counterstained with cresyl fast violet. Inter-animal differences due to variations in incubation procedures were limited by incubating tissue of M11 and M12, and of M14, M15 and M16 simultaneously.

Although ER-β IR was examined with commercially available antisera, the ER-β antibodies did not produce consistently stained tissue. Thus, the data from ER-β staining were not included in this manuscript. At the time of the experiments, the membrane receptor GPR30 had not yet been identified.

Analysis

The brainstem was divided into rostrocaudal levels, at intervals of 1000 μm as described previously (VanderHorst et al., 2000a, VanderHorst et al., 2004). Level zero (level 0) was defined as the level at which the aqueduct of Sylvius opens into the 4th ventricle. The PAG was further subdivided into longitudinal columns as described previously (An et al., 1998, VanderHorst et al., 2000a). For each level, ER-α IR neurons of one section were plotted into one drawing using Neurolucida software (Microbrightfield, Bioscience, Williston, VT, USA) and a Nikon microscope. Counterstained sections and dark field illumination were used to delineate the boundaries of different nuclei and laminae in the brainstem and spinal cord. The methodology used to divide the brainstem into rostrocaudal levels was similar to a recent study on the distribution of ER-α IR neurons in the mouse, allowing for species comparisons (VanderHorst et al., 2005).

For each spinal segment that was examined, ER-α IR neurons of *three* sections were plotted into one drawing, to obtain a better overview of the laminar distribution of immunoreactive neurons (case M18). The graphic data was compiled using Adobe Illustrator 10.0 software. In cases M11, M12, M15, and M18 (all without estrogen administration), the average number of neurons was determined per 50μm transverse section for spinal segments L6 and S1 (n=6 per segment), and the NTS to assess whether significant inter-animal variations were present, and for inter-species comparisons (methodology similar to the mouse: VanderHorst et al., 2005). For the NTS region, statistical difference between the two treatment groups was examined with the t-test (two sample analysis assuming unequal variances) and the significance was attained at $p<0.05$.

Photomicrographs were taken using a Zeiss microscope and Axiovision software. Contrast and brightness were adjusted using Adobe Photoshop 7.0, and the micrographs were labeled using Adobe Illustrator 10.0 software.

Results

ER-α immunoreactivity: experimental conditions

In all cases, ER-α IR neurons were found in restricted regions in the brainstem and spinal cord (Figs. 1, 2, 3 and 4). Among the populations of ER-α IR neurons in these regions, the intensity of labeling varied from light gray to intense black. ER-α IR was primarily restricted to neuronal nuclei, but could also be observed in the cytoplasm surrounding densely stained nuclei when using the H222 primary antibody (Fig. 2). ER-α IR could not be discerned in axons or terminal boutons at the light microscopic level.

The experimental variations were a result of multiple experimental purposes (see material and methods) that allowed us to obtain a maximum amount of data from relatively scarce primate materials. With respect to ER-α antisera used, no major difference was observed in

the distribution pattern of ER-α IR neurons with H222 and 1D5. The intensity of labeling (Fig. 2) was also within similar range. Cytoplasmic staining was observed using the H222 antibody, irrespective of endocrine status or fixative, but not with the 1D5 antibody. The overall distribution pattern of ER-α IR neurons or density of staining was not affected by the concentration of glutaraldehyde in the fixative, and higher concentrations of glutaraldehyde did not correlate with the degree of background staining. Finally, after administration of estradiol, ER-α IR neurons were found in areas similar to the control cases. The density of staining appeared similar in most regions irrespective of estrogen status, except for the NTS in which ER-α IR neurons appeared more intensely stained in cases in which estradiol was administered. The average (±sem) number of ER-α IR neurons per section in the NTS of cases with and without estrogen administration was 26.3±5.7 (n=3) and 16.5±1.3 (n=4), respectively, and these numbers were not statistically different (p=0.12). No differences in distribution pattern or density of staining were seen that could be correlated with short (6 week) or long (>52 week) post-ovariectomy intervals.

Distribution of ER-α IR neurons

Midbrain—The majority of ER-α IR neurons in the brainstem were located in the PAG and the laterally adjacent tegmentum. Within the PAG, ER-α IR neurons were not uniformly distributed (Fig. 1). A large cluster of densely labeled ER-α IR nuclei was present in the ventrolateral (vl) caudal PAG (levels 1, 1.5, and 2 in Fig. 1; Fig. 2B). In the lateral PAG (Fig. 1), large numbers of ER-α IR neurons were present, which were located laterally rather than in the area bordering the aqueduct, especially at levels 3 to 5. ER-α IR nuclei were present throughout the entire rostrocaudal extent of the dorsolateral PAG (especially at levels 5-7) and of the dorsal PAG (especially at levels 3 and 4). Only very few ER-α IR neurons were found in the ventral PAG and dorsal raphe nucleus. Except for densely labeled neurons in the ventrolateral caudal PAG, the labeling intensity of ER-α IR PAG neurons was moderate to weak (Fig. 2).

In the dorsal midbrain at the level of the posterior commissure (level 8), a small group of ER-α IR neurons of moderate intensity was found in the pretectal nucleus (Fig. 1). At this level, another group was located medial to the medial geniculate body in the peripeduncular nucleus (Fig. 2A). This latter group contained moderately to densely stained neurons and extended caudally as far as level 5.

Extending between levels 5 and 2, few, weakly stained ER-α IR neurons were found in the intercollicular nucleus (Fig. 1). More ventrally, weakly stained ER-α IR neurons were present in the cuneiforme nucleus (levels 0 to 2), and lateral pontine tegmentum (levels 0 to 4). A few ER-α IR neurons were present medially in the pontine tegmentum (levels 0 to3). No ER-α IR neurons were found in the dorsal raphe nucleus, rostral and central linear raphe nuclei, nucleus of Edinger-Westphal, substantia nigra, ventral tegmental area, or interpeduncular nucleus. No labeling was found in the ependymal layers lining the PAG or the floor of the 4th ventricle.

Pons and medulla oblongata—Compared to the midbrain, ER-α IR neurons in the pons and medulla oblongata were sparse in number (Fig. 3). The majority of pontine ER-α IR

neurons were present in the lateral parabrachial nucleus (levels 0 and −1; Fig. 3) and in the Kölliker-Fuse area (level 0; Fig. 3). These neurons were moderately to weakly stained. ER-α IR neurons were also present in the pontine central gray, especially medial to the locus coeruleus, but the locus coeruleus appeared devoid of ER-α IR neurons. Between levels −3 and −10, no ER-α IR neurons were found.

In the caudal medulla oblongata (levels -9 to −17; Fig. 3), moderately to densely labeled ER-α IR neurons were found in the commissural nucleus of the nucleus of the solitary tract, almost exclusively caudal to the level of the obex (Fig. 2C; levels −12 to −17, Fig. 3). The superficial and deep laminae of the caudal nucleus of the spinal trigeminal complex caudal to the obex contained lightly labeled ER-α IR neurons (Fig. 3). No ER-α IR neurons were found in the A1 cell group, the area postrema, medullary raphe nuclei, medial or lateral medullary tegmentum.

Spinal cord—ER-α IR neurons were present at all levels of the spinal cord (C3, C7, T2, T12, L2, L4-L7, S1-S3, Figs. 4 and 5). Interestingly, numbers of ER-α IR neurons in the lower lumbar and sacral segments (L6-S3) were much higher than in the cervical, thoracic, and upper lumbar segments (Figs. 4 and 5). The average number of ER-α IR neurons per section for the group that did not receive estrogen treatment (M11, M12, M15, and M18) was 10.5±1.1 (C3; n=2), 21.9±2.7 (C7; n=3), 9.4±0.4 (T2; n=2), 4.1±0.1 (T12; n=3), 15.0±3.6 (L2; n=2), 26.4±2.9 (L4; n=3), 36.5±4.6 (L5; n=3), 44.2±6.1 (L6; n=4), and 62.9±0.8 (L7; n=3), 75.8±9.7 (S1; n=4), 65.6±2.3 (S2; n=3) and 24.2±1.1 (S3; n=3). The number of ER-α IR neurons in the lumbar enlargement (L6) was significantly higher than in the cervical enlargement (C7; p=0.03), and the number in the cervical enlargement (C7) was significantly larger than at T12 (p=0.01).

At all levels, ER-α IR neurons were found in the dorsal horn and area X (Fig. 2 and 4), and the intensity of labeling varied from weak to dense (Fig. 2). Labeled neurons in area X were relatively numerous and represented 37% of the total population of spinal ER-α IR neurons (case M18). From the cervical to mid-lumbar levels, ER-α IR neurons in the dorsal horn were mostly present medially in lamina II, and laterally in lamina V, but labeled neurons were also found in laminae I, III, and IV, leading to a rather scattered distribution pattern (Fig. 4). The numbers of ER-α IR neurons in the spinal dorsal horn at these levels were comparable to those found in the caudal part of the spinal trigeminal nucleus, whereas numbers in the commissural nucleus of the NTS were comparable to those in area X (compare Figs. 3 and 4). In the lower lumbar and sacral segments, in addition to the above pattern of distribution, additional populations of ER-α IR neurons were located in the lateral collateral pathway (Figs. 2 and 4) and more medially in the intermediate zone, including the dorsal commissural nuclei (Figs. 2 and 4). In addition, at (lower) thoracic levels, a few ER-α IR neurons were observed in the intermediolateral cell column (Fig. 4; level 12). No ER-α IR neurons were found in laminae VIII and IX.

Discussion

In the present study, large numbers of ER-α IR neurons were found in the PAG, with smaller populations in the pretectal, peripendicular, cuneiforme, intercollicular nuclei,

parabrachial nuclei, pontine lateral tegmentum, dorsolateral pons medial to the locus coeruleus, commissural nucleus of the NTS, caudal spinal trigeminal nucleus, spinal laminae I-V and area X, thoracic and lumbosacral intermediolateral cell columns and the lumbosacral lateral collateral pathway. The distribution of ER-α IR neurons differs from the distribution of neurons containing ER-β protein or mRNA, which are present in the dorsolateral PAG, dorsal raphe nucleus, substantia nigra, caudal linear nucleus, locus coeruleus and pontine nuclei (Schutzer and Bethea, 1997, Pau et al., 2000, Gundlah et al., 2000, Gundlah et al., 2001, Bethea et al., 2002). The absence of ER-α IR neurons in the dorsal raphe nucleus in macaques is in keeping with findings by Bethea et al. (2002). Differing findings have been reported with respect to the locus coeruleus, in which no significant populations of ER-α IR neurons could be demonstrated in this study as well as in the report by Schutzer and Bethea (1997). However, using *in situ* hybridization, Pau et al. (2000) described ER-α mRNA to be present in neurons of the locus coeruleus, with mRNA levels varying depending on endocrine state. It is possible that ER-α levels were too low for detection with immunohistochemical techniques.

Altogether, the distribution of ER-α IR neurons in the pons, medulla oblongata and spinal cord in the rhesus monkey appears to be less widespread compared to rodent species. We will elaborate on these differences and their implications after a discussion of technical aspects.

Technical considerations

The aim of the present study was primarily to describe the distribution pattern of ER-α IR neurons. However, experimental conditions such as fixative, endocrine status, and anti-sera varied among the experimental cases and might have affected the distribution pattern and/or labeling intensity.

Primary antibodies—With respect to the choice of antibodies, both the H222 and 1D5 antibodies are directed against human ERs, which are highly homologous to ERs in the macaque. H222, which is directed against the C- terminus, has been used previously in the rhesus monkey and the distribution pattern of H222 immunoreactivity was found to overlap with the distribution of ER mRNA (Bethea et al., 1996). Theoretically, the H222 antibody might bind to the ligand-binding domain of ER-β. However, no signal was detected with H222 in the dorsal raphe nucleus, which area in the macaque contains ER-β mRNA and protein, but no ER-α mRNA (Gundlah et al., 2001). In addition, other regions known to contain ER-β mRNA in the rhesus monkey such as the substantia nigra, caudal linear nucleus, and pontine nuclei (Gundlah et al., 2000) did not contain ER-α IR neurons in the present study. In addition, the second antibody against ER-α, 1D5 was used to assess whether the results obtained with the H222 antibody could be reproduced. This antibody is directed against the N-terminus, which area differs between ER-α and ER-β. No differences were observed in the distribution and numbers of ER-IR neurons using H222 and 1D5 as primary antibodies. This is in keeping with studies in rat (Greco et al., 1998) and cat CNS (VanderHorst et al., 2001a). Altogether ER-IR detected in this study most likely represents ER-α IR.

ER-alpha immunoreactivity—Although immunoreactivity was predominantly present in neuronal nuclei, cytoplasmic staining was also observed surrounding densely labeled nuclei. This is in line with previous findings (Blaustein, 1992). Given the variations in experimental conditions, we cannot come to any conclusions with respect to density of labeling among different cases. However, within each single animal, the intensity of staining of ER-α IR neurons varied among different neuronal populations (see below), even when tissue was incubated simultaneously. For example, ER-α IR neurons in the ventrolateral PAG were densely stained, in contrast to labeled neurons in the lateral PAG of the same section. This was the case irrespective of endocrine status, primary antibody, or fixative. Such intra-animal differences in intensity might reflect different levels of ER-α, and/or differential sub-cellular distributions of the receptor and/or differences in affinity of the antibody to the receptor. The intensity of the reaction product in general was relatively low, but the presence of a few intensely stained profiles in most regions as well as intense reaction product in the ventrolateral PAG under the same experimental conditions indicates that the antibody concentrations and incubation periods were sufficient.

Ovariectomy and estrogen treatment—Ovariectomy and estrogen treatment did not significantly alter the distribution pattern of ER-α IR neurons in the midbrain, brainstem and spinal cord. The number of animals included in the present study was too small and the experimental conditions varied too much to provide statistically valid information on possible regional differences related to estrous state. In the primate hypothalamus, estrogen treatment did not affect ER immunoreactivity using the same H222 antibody as used in the present study, and neither did it affect ER mRNA (Bethea at al, 1996). The apparent lack of major differences in results related to estrous state appears to be different for rodent species. For example, in the rat, larger numbers of labeled ER-α IR neurons were found in the A2 cell group in the NTS during proestrous compared to diestrous (Haywood et al., 1999), whereas fewer lumbosacral ER-α IR neurons were described in intact rats compared to ovariectomized rats (Williams and Papka, 1996).

Fixative—No distinct differences in ER-α IR or in background staining were observed when using fixatives with different concentrations of glutaraldehyde. It was expected that higher levels (>0.5%) of glutaraldehyde would severely hamper the penetration of the antibodies into the tissue. Apparently, pretreatment with sodium borohydrate was effective enough to remove excess aldehydes.

The distribution of ER-α IR neurons in the brainstem and spinal cord of the rhesus monkey is different compared to other mammalian species

Qualitative species differences—Each of the regions in which ER-α IR neurons were found in the primate brainstem and spinal cord also contain ER-α mRNA or IR in one or more other species (Table 2). However, many areas that contain ER-α IR neurons in other species are devoid of such neurons in the primate (Table 2). For example, the pons and medulla in the rhesus monkey contain some ER-α IR neurons in the parabrachial nucleus, peri-coeruleus area and in the commissural nucleus of the NTS and a few in the caudal spinal trigeminal nucleus, but other pontomedullary regions are devoid of such neurons in the rhesus monkey. These differences are prominent, especially when comparing the results

of the present study with a study performed in the mouse using similar methodology (VanderHorst et al., 2005; Figures 1 and 4).

Species differences—In addition to a complete absence of ER-α IR neurons in certain regions of the CNS of the primate compared to rodents, species differences also exist with respect to relative numbers of ER-α IR neurons per region. It is difficult to compare numbers of ER-α IR neurons among species and studies. Nonetheless, the present study illustrated prominent species differences in the distribution pattern of ER-α IR neurons.

As discussed above, the PAG contains ER-α IR neurons in all species examined thus far. However, in the monkey ER-α IR neurons were mainly concentrated to the ventrolateral caudal PAG rather than being most abundant in the lateral PAG at intermediate levels as in other species (Simerly et al., 1990, Turcotte and Blaustein, 1993, VanderHorst et al., 1998, Murphy et al., 1999, Vanderhorst et al., 2005). These differences might be functionally significant given the fact that the different columns of the PAG serve different functions (Bandler and Shipley, 1994). In contrast to the relative abundance of ER-α IR neurons in the ventrolateral PAG of the primate, no clusters of ER-α IR neurons were found in the ventral PAG, including the area of the dorsal raphe nucleus, and the A10-dc cell group (compare to mouse: VanderHorst et al., 2005).

Another prominent difference involves ER-α IR neurons in the caudal spinal trigeminal nucleus and spinal cord. Similar to the mouse, spinal ER-α IR neurons in the macaque were most abundant in the lower lumbar and sacral segments (Vanderhorst et al., 2005). However, the numbers in each of the spinal segments in primates was relatively small, ranging from less than a hundred per section for the S1 level to less than 10 for the lower thoracic segments. This is illustrated by the fact that when composing representative drawings of the spinal segments in the primate, the information of *three* 50μm sections had to be combined into one drawing to obtain enough data-points to detect a representative distribution pattern. In contrast, several hundreds of ER-α IR neurons per 40μm section are found in the female ovariectomized mouse (see Figure 5 in VanderHorst et al., 2005). This difference is even more remarkable as the spinal gray matter is much larger in the macaque than in the mouse. Our current data indicate that this difference is primarily due to a paucity of ER-α IR neurons in the primate superficial dorsal horn.

Possible functional roles of ER-α IR neurons in the primate brainstem and spinal cord

Information on the phenotype and afferent and efferent connections of ER-α IR neurons in the primate brainstem and spinal cord is absent, apart from a study demonstrating that ER-α IR neurons in the ventrolateral caudal PAG receive monosynaptic input from the lumbosacral cord (VanderHorst et al., 2002b). In non-primate species it has been shown that populations of ER-α IR neurons are distinct with respect to their afferent and efferent connections and their neurotransmitter content (VanderHorst et al., 2005), as well as to the peptides and growth factors that they express (Merchenthaler et al., 2004).

Given the lack of primate-specific information, we can only speculate on the possible functions of the populations of ER-α IR neurons in the primate brainstem and spinal cord. A major role may be in the modulation of sensory processing and autonomic functions. For

example, ER-α IR neurons in the PAG, Barrington's nucleus (the region medial to the locus coeruleus), parabrachial nucleus, NTS, spinal dorsal horn, spinal area X, thoracic intermediolateral cell column, lumbosacral lateral collateral pathway and parasympathetic nucleus all may modulate visceral (afferent and/or efferent) information. This modulation may take place in the context of sexual behavior, maternal behavior, pregnancy, parturition, or non-gender specific homeostatic functions such as nociception, cardiovascular control, micturition, nausea, food-intake and maintenance of body weight (for a discussion see VanderHorst et al., 2005).

The presence of ER-α IR neurons in the peripeduncular nucleus, brachium of the inferior colliculus, external cortex of the inferior colliculus, and the intercollicular nucleus suggests that ER-α modulates auditory sensory input. This might be important in the context of maternal behavior, which includes the response to vocalization by the infant, or sexual behavior, which includes a response to species specific mating calls. However, compared to non-primate species with larger numbers of ER-α IR neurons in these regions, the role of ER-α in the modulation of these functions may be rather modest.

Possibly one of the more clinically relevant roles of ER-α IR neurons in the primate may involve the modulation of nociception and analgesia. ER-α IR neurons are present in the caudal spinal trigeminal nucleus as well as in the spinal dorsal horn, where they may modulate information from primary afferents conveying nociceptive inputs and/or from descending, modulatory pathways (see Bodnar et al., 2002). Most of all, they are very numerous in the ventrolateral PAG, an area which is involved in opioid dependent analgesia and is known to give rise to descending modulatory pathways. Although it remains unclear how or to what extent gonadal hormones affect different types of pain in primates, including humans (Craft, 2007), there are a few pain syndromes, including migraine headaches, arthritis and temporomandibular disorders, that appear especially susceptible to estrogen (Craft, 2007). Areas that seemed obvious candidates to mediate part of these estrogen actions, such as the spinal trigeminal system for migraine headaches, appear less likely to play a prominent role based on the relative paucity of ER-α IR neurons in this area in the primate compared to rodents. In contrast, the PAG with its abundance of ER-α IR neurons remains of interest. Some physiological data is available in the rhesus monkey on effects of sex steroids on pain modulation. Sex steroids potentiate the anti-nociceptive effects of kappa agonists (Negus and Mello, 2002). However, overall, the influence of gonadal hormones on (somatic) nociception in rhesus monkeys is rather limited (Negus et al., 2004), possibly due to a relative paucity of estrogen receptors in dorsal horn neurons. Based on the relative abundance of ER-α IR neurons in the lumbosacral cord, a more prominent influence of gonadal hormones on nociception may be found in the rhesus monkey when testing nociception mediated by the pelvic and/or pudendal nerves rather than testing for nociceptive stimuli that enter the cord in other regions.

In conclusion, the distribution pattern of ER-α IR neurons in the primate brainstem and spinal cord is species specific and less abundant than in more frequently used rodent models. This difference might reflect the observation that estrogen modulates behavior and neural functions in non-human primates and humans in a more modest way than in rodents. This refers not only to sensory and autonomic aspects of sexual behavior, but also to modulation

of nociception, analgesia and autonomic functions in general. Alternatively, other mechanisms of estrogen action, mediated via ER-β (Gundlah et al., 2000, 2001) or alternative estrogen receptors (Thomas et al., 2005; Revankar et al., 2005; Brailoiu et al., 2007; Abe et al., 2008) might play a more important role in primates.

Acknowledgments

We would like to thank Kim Keen (Wisconsin National Primate Research Center, University of Wisconsin) for her excellent assistance during the surgical part of the experiments, and Toni Milroy, Stephanie Hopkins, and Sandy Canchola (University of California San Francisco) for their assistance with the histological processing.

Support: NS 23347 (to HJR); NIH RR00167 (to ET); Royal Netherlands Academy of Arts and Sciences (KNAW), Foundation “De Drie Lichten”, Netherlands, J.C. De Cock Stichting, Netherlands (to VGJMV).

Literature Cited

Abe H, Keen KL, Terasawa E. Rapid action of estrogens on intracellular calcium oscillations in primate LHRH-1 neurons. Endocrinology. 2008; 149:1155–1162. [PubMed: 18079199]

Alves SE, Weiland NG, Hayashi S, McEwen BS. Immunocytochemical localization of nuclear estrogen receptors and progestin receptors within the rat dorsal raphe nucleus. J Comp Neurol. 1998; 391:322–334. [PubMed: 9492203]

Amandusson A, Hermanson O, Blomqvist A. Estrogen receptor-like immunoreactivity in the medullary and spinal dorsal horn of the female rat. Neurosci Lett. 1995; 196:25–28. [PubMed: 7501248]

An X, Bandler R, Ongur D, Price JL. Prefrontal cortical projections to longitudinal columns in the midbrain periaqueductal gray in macaque monkeys. J Comp Neurol. 1998; 401:455–479. [PubMed: 9826273]

Bandler R, Shipley MT. Columnar organization in the midbrain periaqueductal gray: modules for emotional expression? Trends Neurosci. 1994; 17:379–389. [PubMed: 7817403]

Bethea CL, Brown NA, Kohama SG. Steroid regulation of estrogen and progestin receptor messenger ribonucleic acid in monkey hypothalamus and pituitary. Endocrinology. 1996; 137:4372–4383. [PubMed: 8828498]

Bethea CL, Lu NZ, Gundlah C, Streicher JM. Diverse actions of ovarian steroids in the serotonin neural system. Front Neuroendocrinol. 2002; 23:41–100. [PubMed: 11906203]

Blaustein JD. Cytoplasmic estrogen receptors in rat brain: immunocytochemical evidence using three antibodies with distinct epitopes. Endocrinology. 1992; 131:1336–1342. [PubMed: 1380440]

Blurton-Jones MM, Roberts JA, Tuszynski MH. Estrogen receptor immunoreactivity in the adult primate brain: neuronal distribution and association with p75, trkA, and choline acetyltransferase. J Comp Neurol. 1999; 405:529–542. [PubMed: 10098943]

Bodnar, RJ.; Commons, K.; Pfaff, DW. Central neural states relating pain and sex. Johns Hopkins University Press; Baltimore: 2002.

Boers J, Gerrits PO, Meijer E, Holstege G. Estrogen receptor-alpha-immunoreactive neurons in the mesencephalon, pons and medulla oblongata of the female golden hamster. Neurosci Lett. 1999; 267:17–20. [PubMed: 10400238]

Brailoiu E, Dun SL, Brailoiu GC, Mizuo K, Sklar LA, Oprea TI, Prossnitz ER, Dun NJ. Distribution and characterization of estrogen receptor G protein-coupled receptor 30 in the rat central nervous system. J Endocrinol. 2007; 193:311–321. [PubMed: 17470522]

Chambers KC, Phoenix CH. Differences among ovariectomized female rhesus macaques in the display of sexual behavior without and with estradiol treatment. Behav Neurosci. 1987; 101:303–308. [PubMed: 3606805]

Craft RM. Modulation of pain by estrogens. Pain. 2007; 132(1):S1–S12. [PubMed: 17951005]

Fink G, Sumner BE. Oestrogen and mental state. Nature. 1996; 383:306. [PubMed: 8848040]

Geary N, Asarian L, Korach KS, Pfaff DW, Ogawa S. Deficits in E2-dependent control of feeding, weight gain, and cholecystokinin satiation in ER-alpha null mice. Endocrinology. 2001; 142:4751–4757. [PubMed: 11606440]

Geyer LA, Barfield RJ. Influence of gonadal hormones and sexual behavior on ultrasonic vocalization in rats: I. Treatment of females. J Comp Physiol Psychol. 1978; 92:438–446. [PubMed: 681563]

Greco B, Edwards DA, Michael RP, Clancy AN. Androgen receptors and estrogen receptors are colocalized in male rat hypothalamic and limbic neurons that express Fos immunoreactivity induced by mating. Neuroendocrinology. 1998; 67:18–28. [PubMed: 9485165]

Gundlah C, Kohama SG, Mirkes SJ, Garyfallou VT, Urbanski HF, Bethea CL. Distribution of estrogen receptor beta (ERbeta) mRNA in hypothalamus, midbrain and temporal lobe of spayed macaque: continued expression with hormone replacement. Brain Res Mol Brain Res. 2000; 76:191–204. [PubMed: 10762694]

Gundlah C, Lu NZ, Mirkes SJ, Bethea CL. Estrogen receptor beta (ERbeta) mRNA and protein in serotonin neurons of macaques. Brain Res Mol Brain Res. 2001; 91:14–22. [PubMed: 11457488]

Haywood SA, Simonian SX, van der Beek EM, Bicknell RJ, Herbison AE. Fluctuating estrogen and progesterone receptor expression in brainstem norepinephrine neurons through the rat estrous cycle. Endocrinology. 1999; 140:3255–3263. [PubMed: 10385422]

Herbison AE, Horvath TL, Naftolin F, Leranth C. Distribution of estrogen receptor-immunoreactive cells in monkey hypothalamus: relationship to neurones containing luteinizing hormone-releasing hormone and tyrosine hydroxylase. Neuroendocrinology. 1995; 61:1–10. [PubMed: 7731492]

Keefer DA, Stumpf WE. Atlas of estrogen-concentrating cells in the central nervous system of the squirrel monkey. J Comp Neurol. 1975; 160:419–441. [PubMed: 804499]

Merchenthaler I, Lane MV, Numan S, Dellovade TL. Distribution of estrogen receptor alpha and beta in the mouse central nervous system: In vivo autoradiographic and immunocytochemical analyses. J Comp Neurol. 2004; 473:270–291. [PubMed: 15101093]

Murphy AZ, Shupnik MA, Hoffman GE. Androgen and estrogen (alpha) receptor distribution in the periaqueductal gray of the male Rat. Horm Behav. 1999; 36:98–108. [PubMed: 10506534]

Negus SS, Mello NK. Effects of gonadal steroid hormone treatments on opioid antinociception in ovariectomized rhesus monkeys. Psychopharmacology (Berl). 2002; 159:275–283. [PubMed: 11862360]

Negus SS, Wurrey BA, Mello NK. Sex differences in thermal nociception and prostaglandin-induced thermal hypersensitivity in rhesus monkeys. J Pain. 2004; 5:92–103. [PubMed: 15042517]

Noel SD, Keen KL, Baumann DI, Filardo EJ, Terasawa E. Involvement of G-Protein coupled receptor 30 (GPR30) in rapid action of estrogen in primate LHRH neurons. Submitted to Molecular Endocrinology. 2008

Ogawa S, Chan J, Gustafsson JÅ, Korach KS, Pfaff DW. Estrogen increases locomotor activity in mice through estrogen receptor alpha: specificity for the type of activity. Endocrinology. 2003; 144:230–239. [PubMed: 12488349]

Ogawa S, Eng V, Taylor J, Lubahn DB, Korach KS, Pfaff DW. Roles of estrogen receptor-alpha gene expression in reproduction-related behaviors in female mice. Endocrinology. 1998; 139:5070–5081. [PubMed: 9832446]

Ogawa S, Lubahn DB, Korach KS, Pfaff DW. Aggressive behaviors of transgenic estrogen-receptor knockout male mice. Ann N Y Acad Sci. 1996; 794:384–385. [PubMed: 8853623]

Pau KY, Hess DL, Kohama S, Bao J, Pau CY, Spies HG. Oestrogen upregulates noradrenaline release in the mediobasal hypothalamus and tyrosine hydroxylase gene expression in the brainstem of ovariectomized rhesus macaques. J Neuroendocrinol. 2000; 12:899–909. [PubMed: 10971815]

Pfaff DW, Gerlach JL, McEwen BS, Ferin M, Carmel P, Zimmerman EA. Autoradiographic localization of hormone-concentrating cells in the brain of the female rhesus monkey. J Comp Neurol. 1976; 170:279–293. [PubMed: 825546]

Register TC, Shively CA, Lewis CE. Expression of estrogen receptor alpha and beta transcripts in female monkey hippocampus and hypothalamus. Brain Res. 1998; 788:320–322. [PubMed: 9555076]

Revankar CM, Cimino DF, Sklar LA, Arterburn JB, Prossnitz ER. A transmembrane intracellular estrogen receptor mediates rapid cell signaling. Science. 2005; 307:1625–1630. [PubMed: 15705806]

Saleh MC, Connell BJ, Saleh TM. Autonomic and cardiovascular reflex responses to central estrogen injection in ovariectomized female rats. Brain Res. 2000; 879:105–114. [PubMed: 11011011]

Schutzer WE, Bethea CL. Lack of ovarian steroid hormone regulation of norepinephrine transporter mRNA expression in the non-human primate locus coeruleus. Psychoneuroendocrinol. 1997; 22:325–336.

Sherwin BB. Oestrogen and cognitive function throughout the female lifespan. Novartis Found Symp. 2000; 230:188–196. discussion 196-201. [PubMed: 10965509]

Shughrue PJ, Lane MV, Merchenthaler I. Comparative distribution of estrogen receptor-alpha and -beta mRNA in the rat central nervous system. J Comp Neurol. 1997; 388:507–525. [PubMed: 9388012]

Simerly RB, Chang C, Muramatsu M, Swanson LW. Distribution of androgen and estrogen receptor mRNA-containing cells in the rat brain: an in situ hybridization study. J Comp Neurol. 1990; 294:76–95. [PubMed: 2324335]

Simonian SX, Delaleu B, Caraty A, Herbison AE. Estrogen receptor expression in brainstem noradrenergic neurons of the sheep. Neuroendocrinology. 1998; 67:392–402. [PubMed: 9662719]

Simonian SX, Herbison AE. Differential expression of estrogen receptor and neuropeptide Y by brainstem A1 and A2 noradrenaline neurons. Neuroscience. 1997; 76:517–529. [PubMed: 9015335]

Thomas P, Pang Y, Filardo EJ, Dong Y. Identity of an estrogen membrane receptor coupled to a G protein in human breast cancer cells. Endocrinology. 2005; 146:624–632. [PubMed: 15539556]

Turcotte JC, Blaustein JD. Immunocytochemical localization of midbrain estrogen receptor- and progestin receptor-containing cells in female guinea pigs. J Comp Neurol. 1993; 328:76–87. [PubMed: 8429127]

VanderHorst VG, Gustafsson JÅ, Ulfhake B. Estrogen receptor-alpha and -beta immunoreactive neurons in the brainstem and spinal cord of male and female mice: relationships to monoaminergic, cholinergic, and spinal projection systems. J Comp Neurol. 2005; 488:152–179. [PubMed: 15924341]

VanderHorst VG, Meijer E, Holstege G. Estrogen receptor-alpha immunoreactivity in parasympathetic preganglionic neurons innervating the bladder in the adult ovariectomized cat. Neurosci Lett. 2001a; 298:147–150. [PubMed: 11165428]

VanderHorst VG, Schasfoort FC, Meijer E, van Leeuwen FW, Holstege G. Estrogen receptor-alpha-immunoreactive neurons in the periaqueductal gray of the adult ovariectomized female cat. Neurosci Lett. 1998; 240:13–16. [PubMed: 9488163]

VanderHorst VG, Terasawa E, Ralston HJ 3rd. Monosynaptic projections from the nucleus retroambiguus region to laryngeal motoneurons in the rhesus monkey. Neuroscience. 2001b; 107:117–125. [PubMed: 11744252]

VanderHorst VG, Terasawa E, Ralston HJ 3rd. Axonal sprouting of a brainstem-spinal pathway after estrogen administration in the adult female rhesus monkey. J Comp Neurol. 2002a; 454:82–103. [PubMed: 12410620]

VanderHorst VG, Terasawa E, Ralston HJ 3rd. Estrogen receptor-alpha immunoreactive neurons in the ventrolateral periaqueductal gray receive monosynaptic input from the lumbosacral cord in the rhesus monkey. J Comp Neurol. 2002b; 443:27–42. [PubMed: 11793345]

VanderHorst VG, Terasawa E, Ralston HJ 3rd. Projections from estrogen receptor-alpha immunoreactive neurons in the periaqueductal gray to the lateral medulla oblongata in the rhesus monkey. Neuroscience. 2004; 125:243–253. [PubMed: 15051163]

VanderHorst VG, Terasawa E, Ralston HJ 3rd, Holstege G. Monosynaptic projections from the lateral periaqueductal gray to the nucleus retroambiguus in the rhesus monkey: implications for vocalization and reproductive behavior. J Comp Neurol. 2000a; 424:251–268. [PubMed: 10906701]

VanderHorst VG, Terasawa E, Ralston HJ 3rd, Holstege G. Monosynaptic projections from the nucleus retroambiguus to motoneurons supplying the abdominal wall, axial, hindlimb, and pelvic

floor muscles in the female rhesus monkey. J Comp Neurol. 2000b; 424:233–250. [PubMed: 10906700]

Vasudevan N, Pfaff DW. Non-genomic actions of estrogens and their interaction with genomic actions in the brain. Front Neuroendocrinol. 2008; 29:238–257. [PubMed: 18083219]

Williams SJ, Papka RE. Estrogen receptor-immunoreactive neurons are present in the female rat lumbosacral spinal cord. J Neurosci Res. 1996; 46:492–501. [PubMed: 8950709]

List of abbreviations

3n	oculomotor nerve
3N	oculomotor nucleus
4n	trochlear nerve
4V	fourth ventricle
6N	abducens nucleus
7N	facial nucleus
10N	dorsal motor nucleus of the vagus
12N	hypoglossal nucleus
A1	A1 cell group
Amb	nucleus ambiguus
AP	area postrema
aq	aqueduct
Bar	Barrington's nucleus
BIC	brachium of the inferior colliculus
C3	third cervical segment
C7	seventh cervical segment
CG	central gray
cic	commissure of the inferior colliculus
CN	cochlear nucleus
CnF	cuneiform nucleus
cp	cerebral peduncle
Cu	cuneate nucleus
D	nucleus of Darkschewitz
DCN	dorsal commissural nucleus
df	dorsal funiculus
DH	dorsal horn
dl	dorsolateral

dm	dorsomedial
DR	dorsal raphe nucleus
ECu	external cuneate nucleus
ER-α IR	estrogen receptor-alpha immunoreactive
EW	Edinger-Westphal nucleus
Gr	gracile nucleus
g7	genu of the facial nerve
IC	inferior colliculus
icp	inferior cerebellar peduncle
IML	intermediolateral cell column
IO	inferior olive
IP	interpeduncular nucleus
IVe	inferior vestibular nucleus
KF	Kölliker-Fuse nucleus
l	lateral
L2	second lumbar segment
L4	fourth lumbar segment
L5	fifth lumbar segment
L6	sixth lumbar segment
L7	seventh lumbar segment
LC	locus coeruleus
LCP	lateral collateral pathway
LG	lateral geniculate nucleus
ll	lateral lemniscus
LL	nucleus of the lateral lemniscus
LRt	lateral reticular nucleus
LVe	lateral vestibular nucleus
mcp	middle cerebellar peduncle
Me5	mesencephalic trigeminal nucleus
MG	medial geniculute nucleus
ml	medial lemniscus
mlf	medial longitudinal fasciculus

MnR	median raphe nucleus
MVe	medial vestibular nucleus
NRA	nucleus retroambiguus
NTS	nucleus of the solitary tract
PAG	periaqueductal gray
PBN	parabrachial nucleus
pc	posterior commissure
Pn	pontine nuclei
PnR	pontine raphe nucleus
PP	peripeduncular nucleus
Pr	nucleus prepositus hypoglossi
PT	pretectal nucleus
PUL	pulvinar
py	pyramidal tract
Rli	rostral linear nucleus of the raphe
RMg	nucleus raphe magnus
RN	red nucleus
ROb	nucleus raphe obscurus
RPa	nucleus raphe pallidus
S1	first sacral segment
S2	second sacral segment
S3	third sacral segment
scp	superior cerebellar peduncle
SN	substantia nigra
SO	superior olivary nucleus
Sol	nucleus of the solitary tract
Sp5C	spinal trigeminal nucleus, caudal part
Sp5I	spinal trigeminal nucleus, interpolar part
Sp5O	spinal trigeminal nucleus, oral part
SPN	sacral parasympathetic nucleus
SpVe	spinal vestibular nucleus
Su	superior colliculus

T12	12th thoracic segment
T2	2nd thoracic segment
Tz	nucleus of the trapezoid body
vl	ventrolateral
VTA	ventral tegmental area
xCST	decussation of the corticospinal tract
xscp	decussation of the superior cerebellar peduncle
ZI	zona incerta

Figure 1a

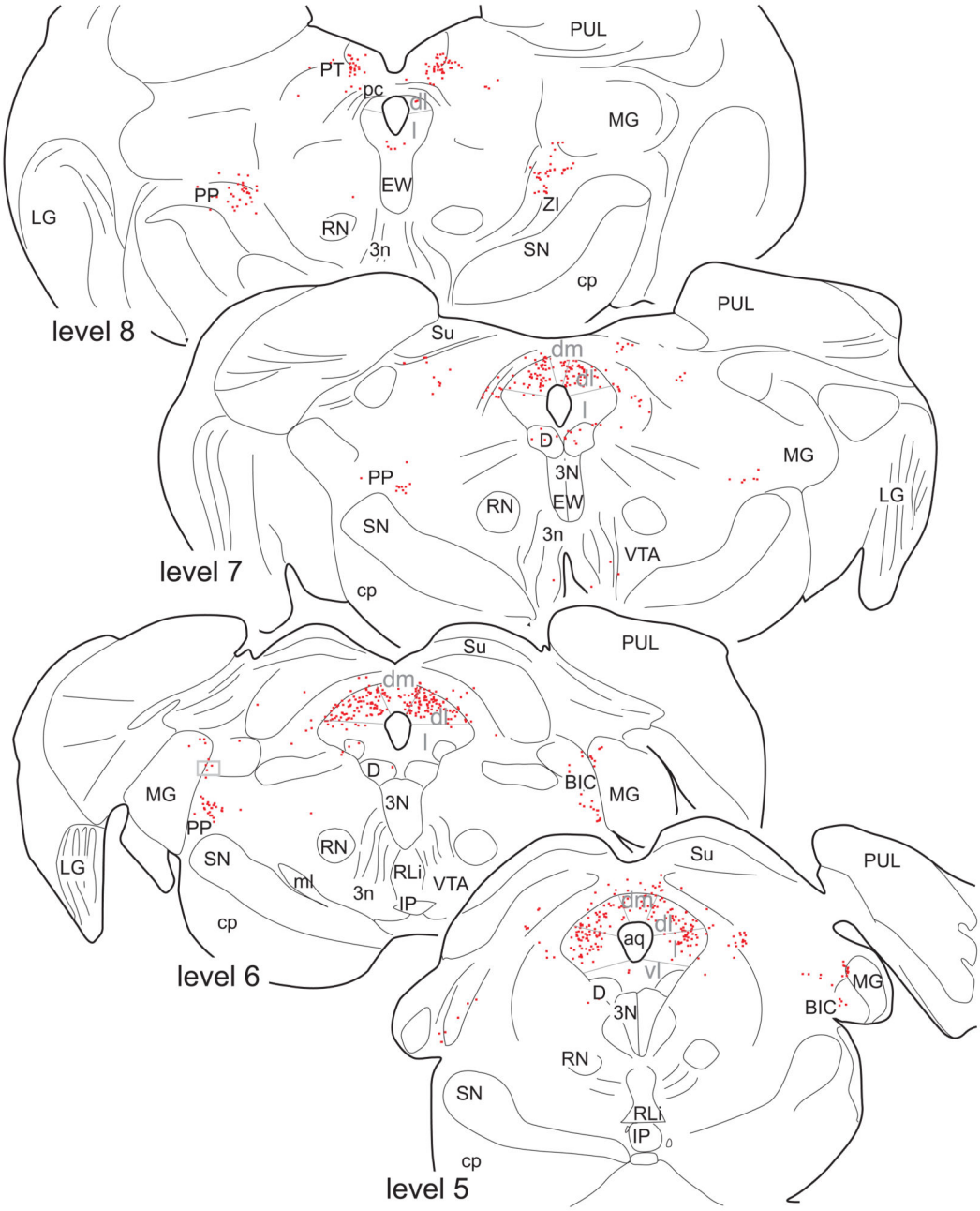

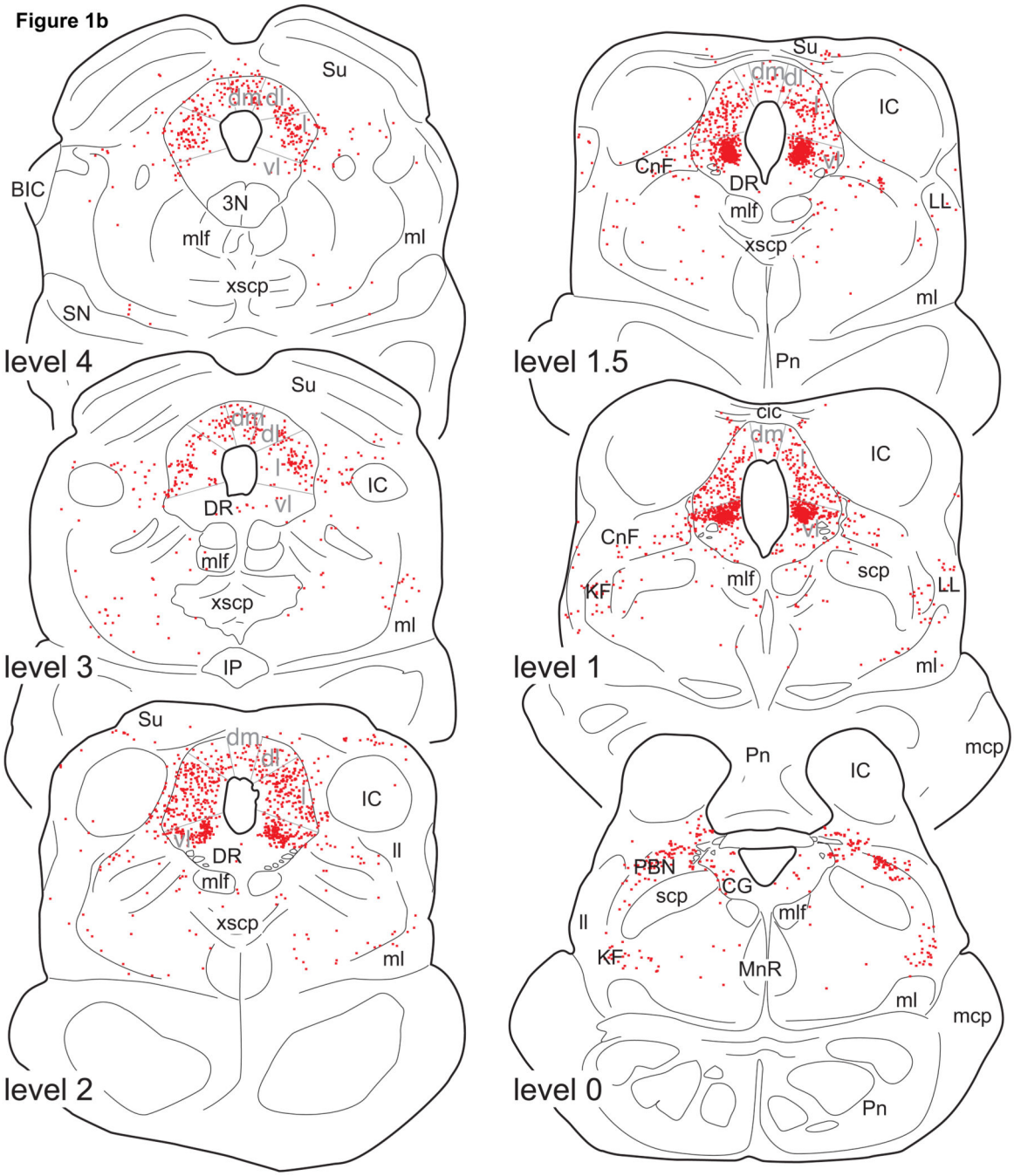

Figure 1.

Line drawings of 50μm thick, transverse sections through the midbrain showing the distribution of ER-α IR neurons in monkey M11. Each dot represents a single ER-α IR neuron. The drawings are taken at intervals of 1mm (levels 8 to 2) or 0.5mm (levels 2, 1.5, and 1). Level 0 is defined as the level at which the aqueduct opens into the 4th ventricle. For abbreviations, see List of Abbreviations.

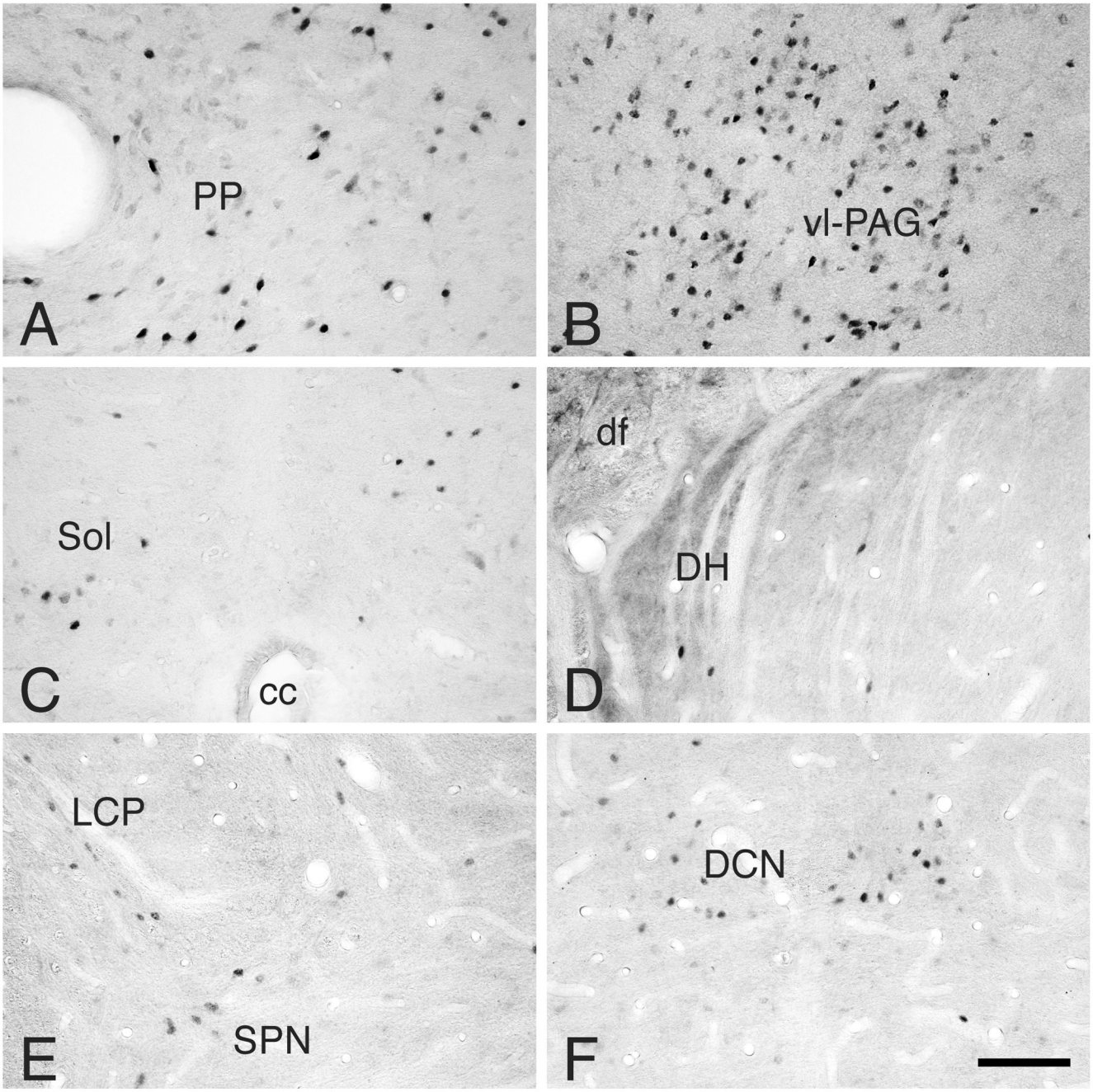

Figure 2.

Photomicrographs of ER-α IR neurons in: A: peripeduncular nucleus, level 6 (M18); B: caudal ventrolateral PAG, level 1.5 (M18); C: commissural nucleus of the Sol, level −15 (M18); D: medial part of the dorsal horn of C7 (M12); E: lateral collateral pathway in S1 (M11); and F: dorsal commissural nucleus of S1 (M11).

Note that ER-α IR neurons are numerous and densely labeled in the peripeduncular area and ventrolateral caudal PAG. ER-α IR neurons in the remaining areas are less numerous and lightly to moderately labeled. For abbreviations, see List of Abbreviations.

Bar: 100μm.

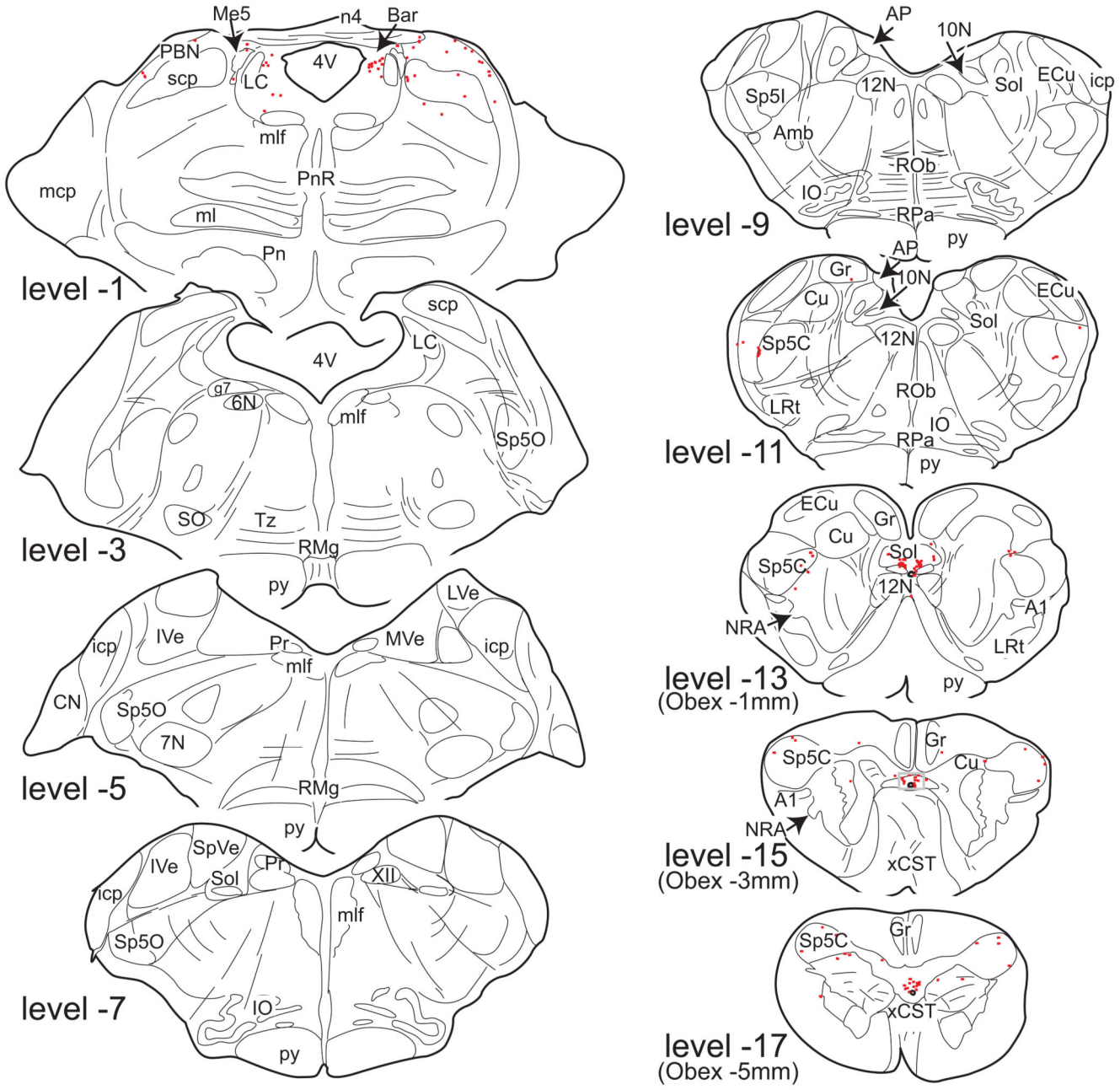

Figure 3.

Line drawings of 50μm thick transverse sections through the pons and medulla oblongata showing the distribution of ER-α IR neurons of monkey M12. Each dot represents a single ER-α IR neuron. The drawings are taken at intervals of 2mm. Level 0 is defined as the level at which the aqueduct opens into the 4th ventricle.

Note that ER-α IR neurons are present only in the dorsolateral pons and caudal medulla oblongata. For abbreviations, see List of Abbreviations.

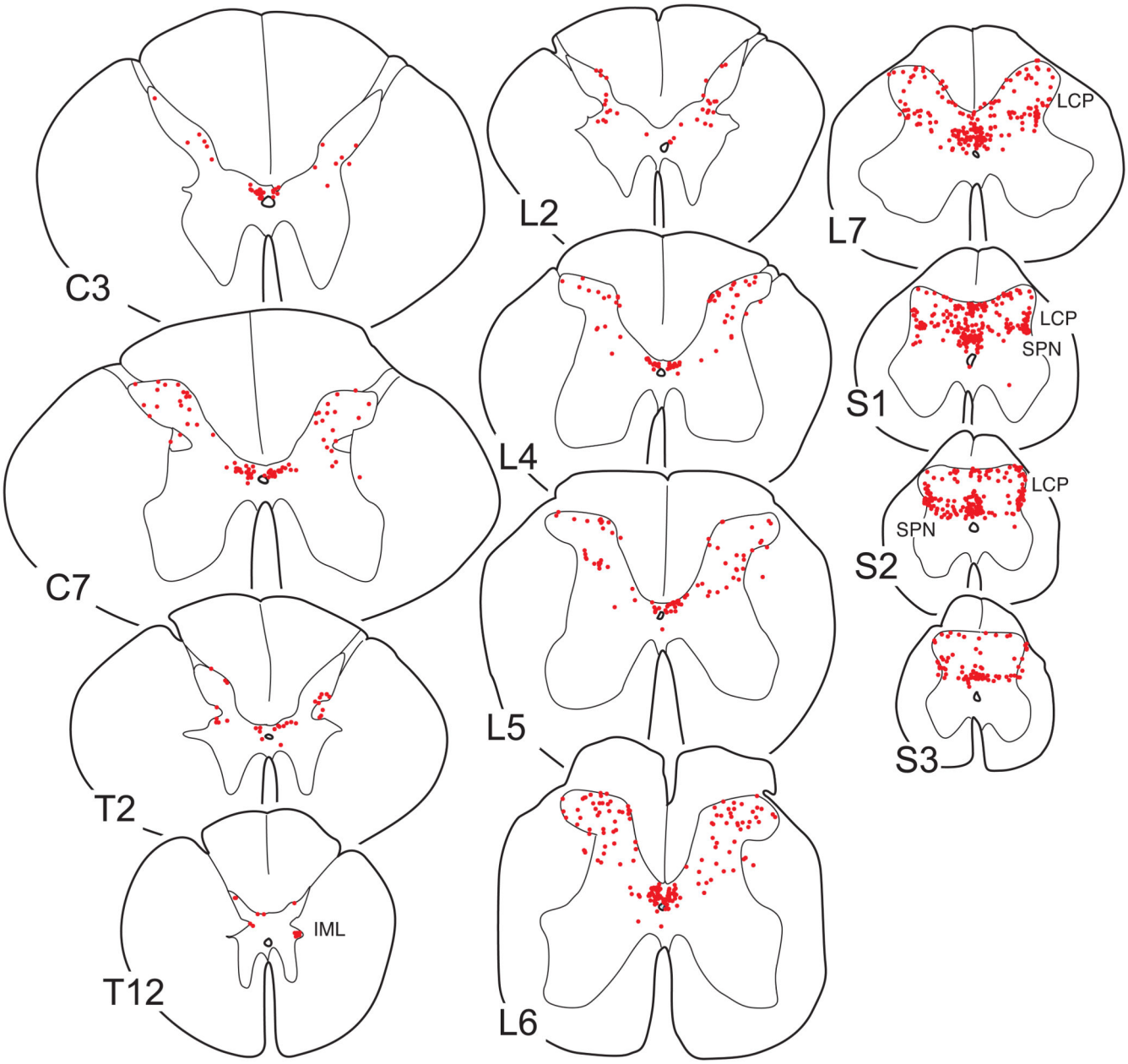

Figure 4.

Line drawings of 50μm thick transverse sections through different spinal segments showing the distribution of ER-α IR neurons in monkey M18. In contrast to figures 1 and 3, each drawing is composed of *three* 50μm sections to obtain a better overview of the laminar distribution. Each dot represents a single ER-α IR neuron. For abbreviations, see List of Abbreviations.

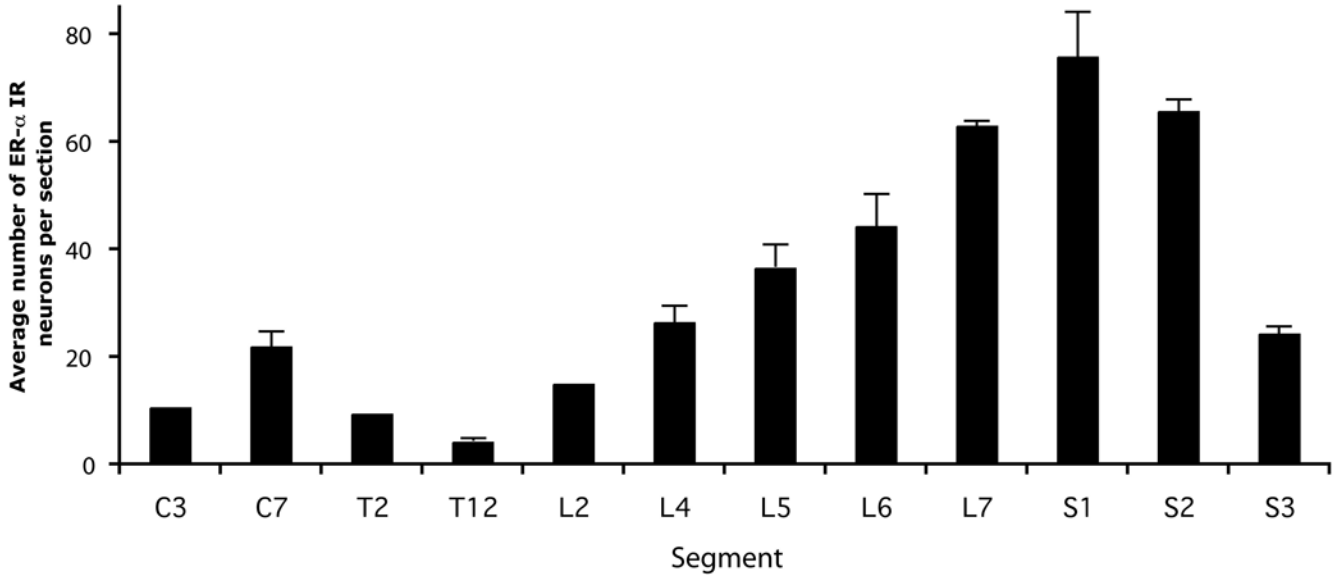

Figure 5.

Graphs showing the segmental distribution of spinal ER-α IR neurons in monkeys that did not receive estrogen treatment. The average number of ER-α IR neurons per 50μm transverse section is depicted, as determined in six non-adjacent transverse sections per segment per case (M12, M18: all segments; M15: all segments except C3, T2 and L2; M11: segments L6 and S1). SEM is indicated only for data that represents more than 2 animals.

Table 1

Overview of experimental parameters

Case	Age (yrs)	OVX (wks)	Estradiol Benzoate	Fixative	Primary Antibody
M11	18	6	no	4%PF, 0.5% GA	H222
M12	12	6	no	4%PF, 0.5% GA	H222
M14	8	>52	yes	1.5%PF, 1.5% GA	H222
M15	10	>52	no	1.5%PF, 1.5% GA	H222
M16	11	12	yes	1.5%PF, 1.5% GA	H222
M17	18	12	yes	1.5%PF, 1.5% GA	H222
M18	26	none	no	4%PF	1D5

OVX: ovariectomy, interval between ovariectomy and perfusion

GA: glutaraldehyde

PF: paraformaldehyde

Table 2

Overview of major regional differences in the distribution of ER-α IR or mRNA expressing neurons in the brainstem and spinal cord among various species

	Macaque	Guinea Pig	Rat	Mouse	Hamster	Cat	Sheep
Pretectal nucleus	+	+*	NA	+	-	NA	NA
Peripeduncular nucleus	+	+	+	+	+	NA	NA
Periaqueductal gray	+	+	+	+	+	+	NA
Cuneiforme nucleus	+	+	+	+	-	+	NA
A10-dc	-	NA	NA	+	NA	NA	NA
Dorsal raphe nucleus	-	+*	+	+	-	-	NA
Deep mesencephalic nuclei	-	+	+	+	-	+	NA
Parabrachial nucleus	+	+	+	+	+	+	+
Locus coeruleus	+/-	NA	+	+	-	NA	-
Reticulotegmental nucleus	-	+*	NA	+	-	NA	-
Barrington's nucleus	+	NA	NA	+	-	NA	+*
Pontine lateral tegmentum	+	+	+	+	-	NA	-
Caudal spinal trigeminal nucleus	+	NA	+	+	-	NA	+
Nucleus of the solitary tract	+	NA	+	+	+	NA	+
Lateral medullary tegmentum	-	NA	-	+	+	NA	+
A1 cell group	-	NA	+	+	+*	NA	+
Area postrema	-	NA	+	+	-	NA	+
Spinal dorsal horn	+	NA	+	+	NA	+	NA
Area X	+	NA	+	+	NA	+	NA
Thoracic intermediolateral cell column	+	NA	-	+	NA	NA	NA
Sacral lateral collateral pathway	+	NA	+	+	NA	+	NA
Sacral parasympathetic region	+	NA	+	+	NA	+	NA

+: present per text

- : absent per text

+*: present based on figures, but data not mentioned in the text

+/-: contradictive reports

NA: no data available

Please note that this overview does not reflect species specific quantitative differences (Macaque: Schutzer and Bethea, 1997; present study; VanderHorst et al., 2002b, 2004; Pau et al., 2000; Guinea Pig: Turcotte and Blaustein, 1993; Rat; Simerly et al., 1990; Amandusson et al., 1995; Williams and Papka, 1996; Shughrue et al., 1997; Alves et al., 1998; Haywood et al., 1999, Murphy et al., 1999; Mouse: Merchenthaler et al., 2004; VanderHorst et al., 2005; Hamster: Boers et al., 1999; Cat: VanderHorst et al., 1998; VanderHorst et al., 2001a; Sheep: Simonian and Herbison, 1997; Simonian et al., 1998).